Enhanced electron field emission from ZnO nanoparticles-embedded DLC films prepared by electrochemical deposition

Peizeng Zhang [a], Ruishan Li [b], Hua Yang [b], Youcai Feng [b], Erqing Xie [a,*]

[a] Key Laboratory for Magnetism and Magnetic Materials of the Ministry of Education, Lanzhou University, Lanzhou 730000, People's Republic of China
[b] School of Science, Lanzhou University of Technology, Lanzhou 730050, People's Republic of China

A B S T R A C T

ZnO nanoparticles-embedded diamond-like amorphous (DLC) carbon films have been prepared by electrochemical deposition. Transmission electron microscopy (TEM) and high-resolution TEM (HRTEM) results confirm that the embedded ZnO nanoparticles are in the wurtzite structure with diameters of around 4 nm. Based on Raman measurements and atomic force microscope (AFM) results, it has been found that ZnO nanoparticles embedding could enhance both graphitization and surface roughness of DLC matrix. Also, the field electron emission (FEE) properties of the ZnO nanoparticles-embedded DLC film were improved by both lowering the turn-on field and increasing the current density. The enhancement of the FEE properties of the ZnO-embedded DLC film has been analyzed in the context of microstructure and chemical composition.

1. Introduction

Diamond-like carbon (DLC) films are considered as good electron emitters for field emission displays due to negative electron affinity, high thermal conductivity and chemical inertness [1]. Although DLC films exhibit comparatively good field electron emission (FEE) performance, the use of DLC films as cold cathode materials is limited by the shortcomings of high compressive stress and low conductivity [2]. One of the strategies to enhance the FEE characteristics is to incorporate other elements into DLC films. It has been reported that the FEE properties of DLC films could be improved by both lowering the turn-on field and increasing the current density after the incorporation of various elements, such as Ti, S, N, and Si [3,4].

Zinc oxide (ZnO), an n-type semiconductor with a wide bandgap (3.37 eV) and a large exciton binding energy (60 meV), has drawn renewed attention due to its promising integration into optoelectronic devices, sensors, spintronics and so on [5]. Moreover, ZnO nanostructures have started to emerge as very promising FEE materials because of their high aspect ratios, negative electron affinity and chemical stability [6]. Tseng et al. reported the FEE current density of 0.1 mA/cm^2 from ZnO nanorods achieved at an

applied voltage of 24 V/μm [7]. However, the Young's modulus value of bulk ZnO is only about 110 Gpa, and such lower Young's modulus value could bring a series of problems of not being able to fully utilize ZnO in applications whereby good mechanical properties are generally desired. Hence, there is a strong demand to study the feasibility of embedding ZnO nanostructures within hard protective materials, such as DLC films. By embedding ZnO nanoparticles within the DLC films, DLC matrix could act as a protective coating to improve the mechanical properties of ZnO nanoparticles. Hsieh et al. has reported the incorporation of ZnO into DLC film by Filtered Cathodic Vacuum Arc (FCVA) technique, and found that the Young's modulus of the embedded ZnO nanoclusters was higher than that of the bulk ZnO [8]. Furthermore, the resistance and compressive stress of the DLC films could be decreased by the ZnO nanoparticles embedding, and hence the FEE properties could be enhanced. Combining ZnO nanoparticles with DLC matrix is expected to provide the advantages of both materials in the FEE properties.

In this work, ZnO nanoparticles were embedded within DLC films by electrochemical deposition. Method for DLC fabrication based on electrochemical deposition has demonstrated such advantages as the relative simple equipment required, low production cost and the possibility of doping by various elements [9,10]. We investigate the FEE properties of DLC and ZnO-embedded DLC (ZnO–DLC) films in the context of microstructure and chemical composition.

* Corresponding author. Tel.: +86 13893337337; fax: +86 9318913554.
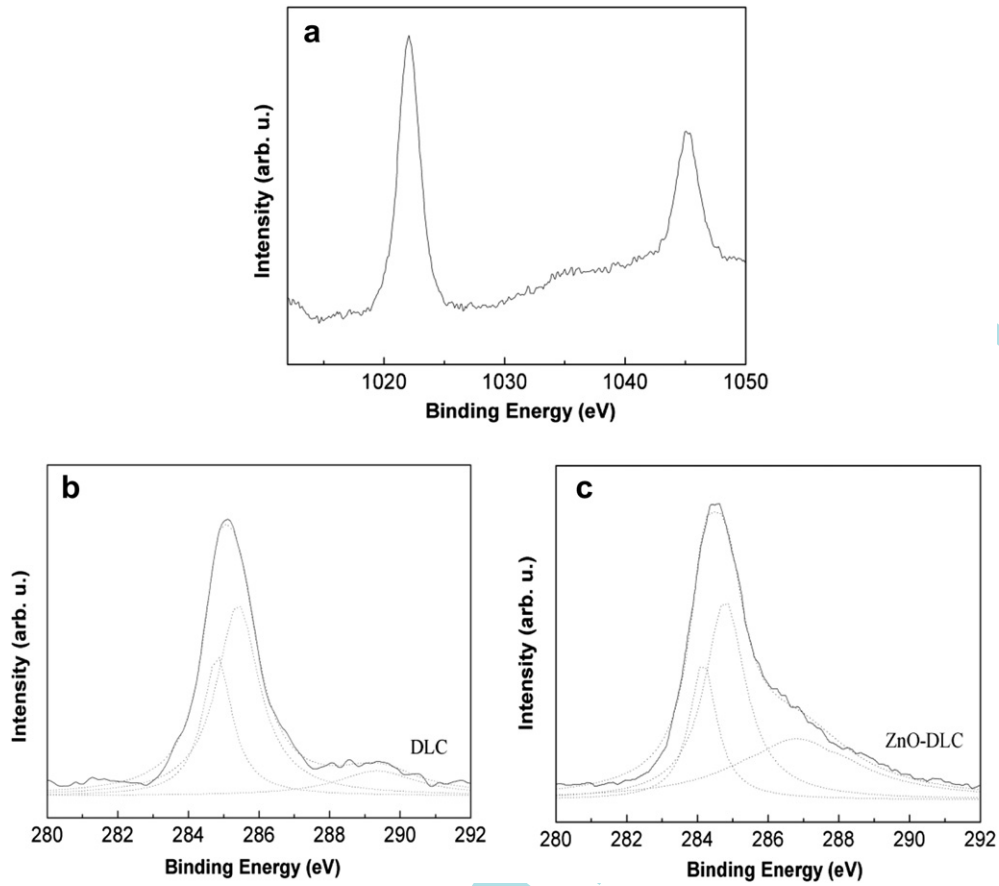*E-mail addresses:* zhangpz09@lzu.cn (P. Zhang), xieeq@lzu.edu.cn (E. Xie).

Fig. 1. The Zn2p XPS spectrum of DLC film (a). The deconvoluted C1s XPS spectra of DLC (b) and ZnO-DLC (c) films.

2. Experimental

The DLC and ZnO–DLC films were fabricated using an electrolytic cell system described in detail in Ref. [9]. An n-type (100) silicon substrate ($10 \times 20 \times 1$ mm^3) with a sheet resistance of around 7–13 Ω/cm^2 was mounted on the negative electrode, and a platinum foil electrode was used as anode with a distance of 7 mm to the cathode. For ZnO embedding, an organic compound $Zn_2[C_{32}H_{42}N_8O_{13}]Cl_{44}$ was served as zinc source. The electrolytic solution was prepared by dissolving $Zn_2[C_{32}H_{42}N_8O_{13}]Cl_4$ in analytically pure methanol with the concentration of 0.08 g/ml. The voltage between two electrodes was fixed at 1000 V. During the deposition process, the temperature was controlled around 50–60 °C. The deposition process was lasted for 8 h. In order to investigate the effects of ZnO embedding on the FEE properties of DLC films, DLC films were electrodeposited using the electrolyte of pure methanol under the same experimental conditions for comparison.

The chemical states of the typical elements of the samples were examined by X-ray photoelectron spectroscopy (XPS, Perlin–Elmer PHI-5702). The Raman measurements were carried out on a Jobin–Ivon LabRam HR800 Raman apparatus with a laser source wavelength of 532 nm. Additional structural characterization was carried out using transmission electron microscopy (TEM, JEM-1200EX). The surface morphologies of the films were examined using atomic force microscope (AFM, CSPM4000). The FEE properties of the films were measured in a parallel plate configuration with a stainless steel anode at a pressure of $\sim 10^{-6}$ Torr. The anode–cathode distance was 100 μm. The testing area was 4.15 mm^2. The applied
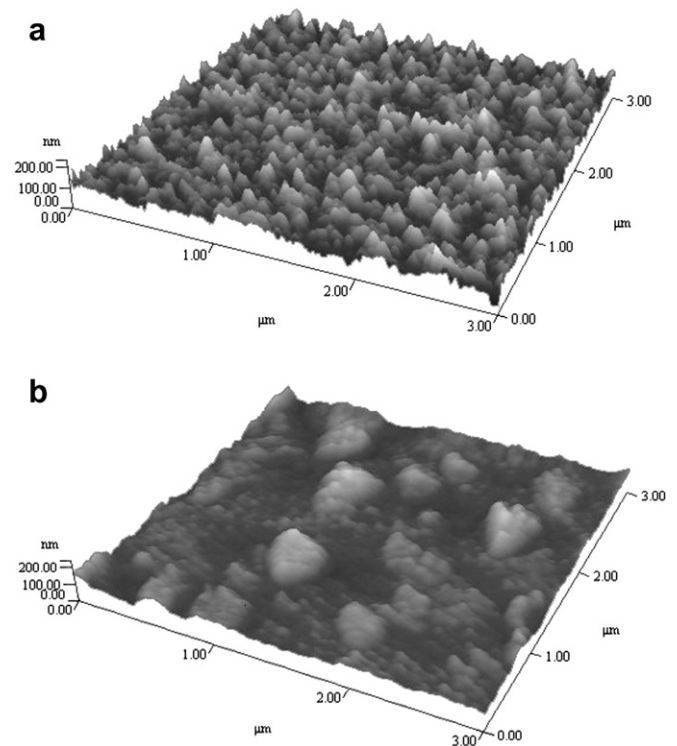

Fig. 2. The 3D AFM surface micrographs of DLC (a) and ZnO-DLC (b) films.
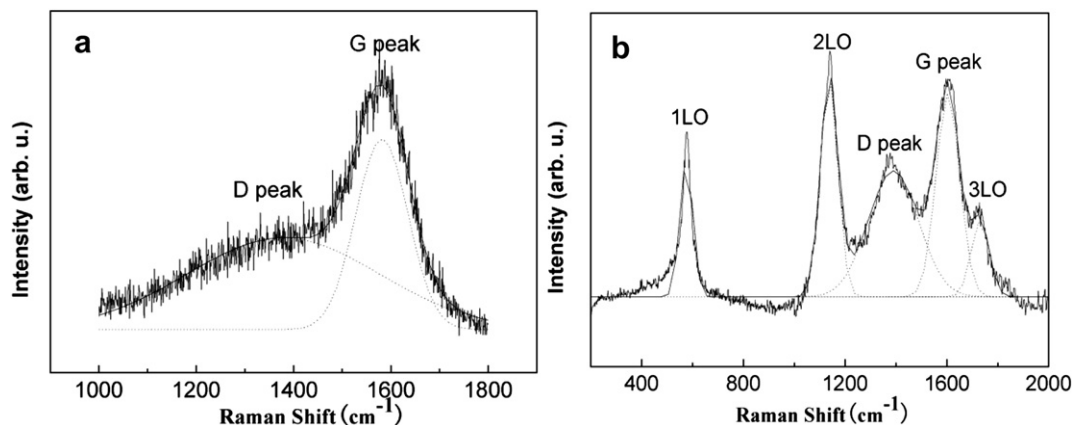
Fig. 3. The Raman spectra of (a) DLC and (b) ZnO-DLC films.

voltage was gradually increased from 0 to 2350 V. The electric field is defined using a formula $E = V/d$ (V is the applied voltage and d is anode-to-cathode separation). The field emission current density is defined using the formula $J = I/S$ (I is the field emission current and S is the entire area of samples exposed to the anode screen).

3. Results and discussion

The chemical composition of DLC and ZnO–DLC films electro-chemically deposited on Si substrates was investigated by XPS. The survey spectrum of a DLC film indicate that the film contains mainly carbon and a small amount of oxygen, while the ZnO–DLC film contains 8.9 at% zinc besides 80.1 at% carbon and 11.0 at% oxygen, suggesting that Zn element has been successfully doped into DLC films. The appearance of the O 1 s peak, which is common for the spectra of this kind of films, might be designated to the contamination of the samples for the exposure to air and the absorption in the deposition process [11]. For further clarifying the chemical bonds in the films, the binding energies of Zn_{2p} and C_{1s} are illustrated in Fig. 1. As evidenced in Fig. 1 (a), the Zn_{2p} peaks of the ZnO–DLC film present the binding energies of $Zn_{2p1/2}$ and $Zn_{2p3/2}$ at around 1045.4 eV and 1022.4 eV, respectively, coinciding with the characteristics of ZnO [12]. This demonstrates that the Zn atoms are bonded to O atoms instead of C atoms in the films. The binding energies of the C1s peaks of DLC and ZnO–DLC samples both range between 284.5 and 285.5eV, as shown in Fig. 1 (b) and (c). The spectra were fitted with three peaks obtained at 284.2–284.7, 285.2–285.7 and 286.8–289.2eV, which have been assigned to graphite (284.4 eV), diamond (285.2 eV) and CO-contaminated, respectively. Since the area of each peak is directly related to the concentration of the corresponding phase, the sp^3 content could be estimated by taking the ratio of diamond peak area over the sum of diamond and graphite peak areas. It has been found that the doping of ZnO decreased the sp^3 content from 0.67 of the DLC sample to 0.61 of the ZnO–DLC sample. This can be interpreted in terms of the graphitization of the DLC matrix induced by ZnO dopping. Fig. 2 (a) and (b) show the 3D AFM surface micrographs of DLC and ZnO–DLC films, respectively. As evidenced in Fig. 2, the ZnO–DLC film exhibits a relatively rougher surface with an rms roughness of 76 nm than that of the DLC film with an rms roughness of 35 nm.

Apparently, ZnO doping greatly changed the intrinsic structure of amorphous carbon films, which could be further analyzed by Raman analysis. Raman spectra of DLC and ZnO–DLC films are given in Fig. 3 (a) and (b), respectively. Obviously, the main characteristics of D band, corresponded to the breathing modes of sp^2 ring structure in disorder graphite, and G band, attributed to E_{2g} vibration mode arising from the bond stretching of all pairs of sp^2 atoms in both rings and chains, both appear in the range of 1200^{-1}–1700 cm^{-1} for the two samples, indicating the existence of mixed sp^2 and sp^3 bonding in the deposited films [1]. In order to further clarify the microstructure characteristics of the samples,
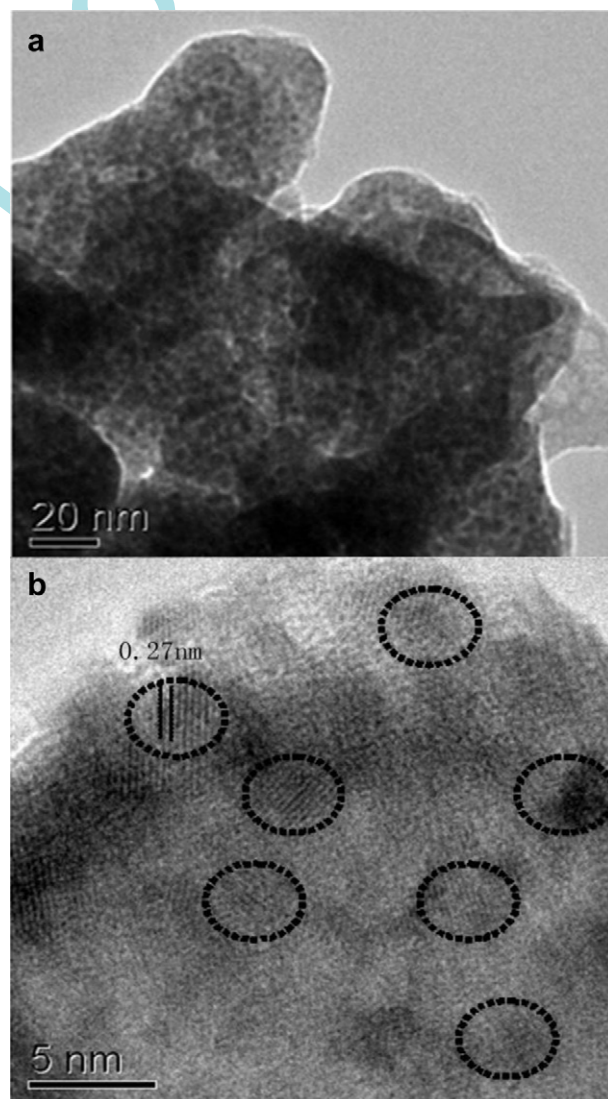

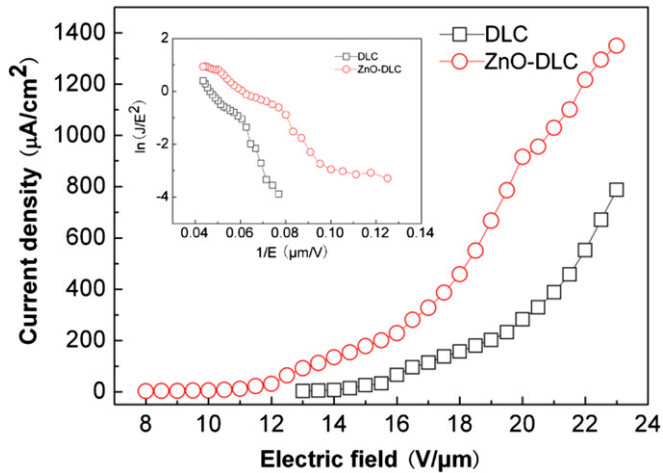**Fig. 4.** The TEM (a) and HRTERM (b) images of the ZnO-DLC film.

Fig. 5. *J—E* curves of DLC and ZnO-DLC films. The inset curves are the corresponding F—N plots.

Raman spectra were further fitted in the Guassian mode. Fig. 3 (a) shows two peaks as G peak at around ~1580 cm^{-1} and D peak at around ~1350 cm^{-1}, with an integrated intensity ratio I(D)/I(G) of 0.58. For the composite ZnO—DLC film, as shown in Fig. 3 (b), compared with those of the DLC film, both D and G peaks move to higher wavenumbers and the I(D)/I(G) increases to 0.76. This is attributed to the graphitization of DLC matrix resulted from ZnO embedding. In addition to D and G peaks, a number of LO multi-phonon peaks corresponding to ZnO nanoparticles are observed in the Raman spectrum of the ZnO—DLC film. The peak at 577 cm^{-1} is related to longitudinal optical (LO) phonon mode of ZnO nano-particles. In the high-frequency region, LO overtones and combi-nations involving LO modes induce a second-order feature peak near 1140 cm^{-1} [13]. However, the strength of the observed peak is too intensive to be caused by the LO peak of ZnO only. The possible explanation should take the *v*1 mode of *trans*polyacetylene (*trans*-PA) in the DLC matrix into account.

Fig. 4(a) and (b) shows the TEM and HRTEM images of the ZnO—DLC composite film, respectively. The spherical ZnO nano-particles (dark spots) with diameters of around 4 nm were uniformly embedded in amorphous carbon matrix (bright area), and show no agglomeration. This may interpreted the rougher surface of the ZnO—DLC film observed by AFM. During the depo-sition process, the inhomogeneity of film-forming associated with ZnO doping may induce the increase of surface roughness of the DLC film. In the HRTEM image, the lattice spacings between adja-cent lattice planes are approximately 0.27 nm, in agreement with the distance between two (002) crystal planes of hexagonal wurt-zite structured ZnO [13], confirming that the ZnO nanoparticles embedded in the DLC film are in a wurtzite structure.

Fig. 5 presents the FEE curves of DLC and ZnO—DLC films. It can be seen that the FEE current density from the ZnO—DLC film is higher than that from the DLC film. In addition, the turn-on field, under which a 2.5 μA/cm^2 current density is extracted, is reduced from 13.5 V/μm for the DLC film to 7 V/μm for the ZnO—DLC composite film. The figure reveals that the highest current

density is about 1.5 mA/cm^2 at the electric field of 23.5 V/μm from the ZnO—DLC film. The possible reason for the above observations is the joint effect of surface roughness and microstructure variation. Previous AFM studies of DLC and ZnO—DLC films have indicated that the embedded ZnO nanoparticles induce surface protrusions on the ZnO—DLC film, which could act as a source of geometric field enhancement. Simultaneously, ZnO embedding enhances the graphitization of DLC matrix. It is known that sp^2-bonded carbon would form conducting channels and provide sufficient electrons to the sp^3-bonded carbon acting as emission sites. The presence of abundant sp^2-bonded carbon may advantage the current forming and flowing in the film.

The emission current is determined by the Fowler—Nordheim (FN) equation [14]:

$$J = A(\beta E)^2 \exp\left(- B\varphi^{3/2}/\beta E\right)$$

where *J* is the emission current density, *φ* is the work function called the emission barrier, *E* is the electric field, and *β* is the field enhancement factor at sharp geometries. By ploting ln(J/E^2) against (1/E), the inset shows the corresponding FN plots of the sample. Assuming the field enhancement factor *β* to be 1, the slopes of the plots give barriers of 69 and 43 meV for DLC and ZnO—DLC films, respectively. Actually, the real value of the work function should be larger because of the underestimation of the field enhancement factor *β*.

4. Conclusion

ZnO nanoparticles with a wurtzite structure were embedded within DLC films by electrochemical deposition. The embedding of ZnO nanoparticles could enhance both surface roughness and graphitization of the DLC films. The FEE properties of the ZnO—DLC films have been improved with the turn-on field fall and the FEE current density rise by ZnO embedding. The results show that the electrochemical deposited ZnO—DLC composite films can be a promising candidate as field emission emitters.

References

[1] J. Robertson, Surf. Coat. Technol. 50 (1992) 185—203.
[2] S.R.P. Silva, J.D. Carey, X. Guo, W.M. Tsang, C.H.P. Poa, Thin Solid Films 482 (2005) 79—85.
[3] S.F. Ahmed, M.K. Mitra, K.K. Chattopadhyay, Appl. Surf. Sci. 253 (2007) 5480—5484.
[4] R. Paul, S. Dalui, A.K. Pal, Surf. Coat. Technol. 204 (2010) 4025—4033.
[5] L. Wang, N.C. Giles, J. Appl. Phys. 94 (2003) 973—978.
[6] C.J. Lee, T.J. Lee, S.C. Lyu, Y. Zhang, H. Ruh, H.J. Lee, Appl. Phys. Lett. 81 (2002) 3648—3650.
[7] Y.K. Tseng, C.J. Huang, H.M. Cheng, I.N. Lin, K.S. Liu, I.C. Chen, Adv. Funct. Mater. 13 (2003) 811—814.
[8] J. Hsieh, D.H.C. Chua, B.K. Tay, E.H.T. Teo, M. Tanemura, Diamond Relat. Mater. 17 (2008) 167—170.
[9] Y. Namba, J. Vac. Technol. A10 (5) (1992) 3368—3370.
[10] S. Kundoo, P. Saha, K.K. Chattopadhyay, Mater. Lett. 58 (2004) 3920—3924.
[11] X.B. Yan, T. Xu, G. Chen, H.W. Liu, S.R. Yang, Carbon 42 (2004) 3103.
[12] D.R. Jung, D. Son, J. Kim, C. Kim, B. Park, Appl. Phys. Lett 93 (2008) 1—3 163118.
[13] Ramon Cuscó, Esther Alarcón-Lladó, Jordi Ibáñez, Luis Artús, Phys. Rev. B 75 (2007) 1—11 165202.
[14] R.H. Fowler, L.W. Nordheim, Proc. Roy. Soc. A 119 (1928) 173—181.